

## WHERE ARE THE MISSING GALACTIC SATELLITES?

ANATOLY A. KLYPIN, ANDREY V. KRAVTSOV, AND OCTAVIO VALENZUELA

Astronomy Department, New Mexico State University, Box 30001, Dept. 4500, Las Cruces, NM 88003-0001

FRANCISCO PRADA

Instituto de Astronomia, Apartado Postal 877, 22900 Ensenada, Mexico

*submitted to the Astrophysical Journal*

### ABSTRACT

According to the hierarchical clustering scenario, galaxies are assembled by merging and accretion of numerous satellites of different sizes and masses. This ongoing process is not 100% efficient in destroying all of the accreted satellites, as evidenced by the satellites of our Galaxy and of M31. Using published data, we have compiled the circular velocity ( $V_{\text{circ}}$ ) distribution function (VDF) of galaxy satellites in the Local Group. We find that within the volumes of radius of 570 kpc ( $400 h^{-1}$  kpc assuming the Hubble constant<sup>a</sup>  $h = 0.7$ ) centered on the Milky Way and Andromeda, the average VDF is roughly approximated as  $n(> V_{\text{circ}}) \approx 45(V_{\text{circ}}/10 \text{ km s}^{-1})^{-1} h^3 \text{Mpc}^{-3}$  for  $V_{\text{circ}}$  in the range  $\approx 10 - 70 \text{ km s}^{-1}$ . The observed VDF is compared with results of high-resolution cosmological simulations. We find that the VDF in models is very different from the observed one:  $n(> V_{\text{circ}}) \approx 1200(V_{\text{circ}}/10 \text{ km s}^{-1})^{-2.75} h^3 \text{Mpc}^{-3}$ . Cosmological models thus predict that a halo of the size of our Galaxy should have about 50 dark matter satellites with circular velocity  $> 20 \text{ km s}^{-1}$  and mass  $> 3 \times 10^8 M_{\odot}$  within a 570 kpc radius. This number is significantly higher than the approximate dozen satellites actually observed around our Galaxy. The difference is even larger if we consider abundance of satellites in simulated galaxy groups similar to the Local Group. The models predict  $\sim 300$  satellites inside a 1.5 Mpc radius, while there only  $\sim 40$  satellites are observed in the Local Group. The observed and predicted VDFs cross at  $\approx 50 \text{ km s}^{-1}$ , indicating that the predicted abundance of satellites with  $V_{\text{circ}} \gtrsim 50 \text{ km s}^{-1}$  is in reasonably good agreement with observations.

We conclude, therefore, that unless a large fraction of the Local Group satellites has been missed in observations, there is a dramatic discrepancy between observations and hierarchical models, regardless of the model parameters. We discuss several possible explanations for this discrepancy including identification of some satellites with the High Velocity Clouds observed in the Local Group, and the existence of dark satellites that failed to accrete gas and form stars due either to the expulsion of gas in the supernovae-driven winds or to gas heating by the intergalactic ionizing background.

<sup>a</sup>Assuming  $H_0 = 100h \text{ km s}^{-1} \text{Mpc}^{-1}$ .

*Subject headings:* cosmology: theory – galaxy formation – methods: numerical

### 1. INTRODUCTION

Satellites of galaxies are important probes of the dynamics and masses of galaxies. Currently, analysis of satellite dynamics is one of the best methods of estimating the masses within large radii of our Galaxy and of the Local Group (e.g., Einasto & Lynden-Bell 1982; Lynden-Bell et al. 1983; Zaritsky et al. 1989; Fich & Tremaine 1991), as well as the masses of other galaxies (Zaritsky & White 1994; Zaritsky et al. 1997). Although the satellites of the Milky Way and Andromeda galaxy have been studied for a long period of time, their number is still uncertain. More and more satellites are being discovered (Irwin et al. 1990; Whiting et al. 1997; Armandroff et al. 1998; Karachentseva & Karachentsev 1998) with a wide range of properties; some of them are relatively large and luminous and have appreciable star formation rates (e.g., M33 and the Large Magellanic Cloud; LMC). Exempting the strange case of IC10, which exhibits a high star formation rate ( $0.7 M_{\odot} \text{yr}^{-1}$ ; Mateo 1998), most of the satellites are dwarf spheroidals and dwarf ellipticals with signs of only mild star-formation of  $10^{-3} M_{\odot} \text{yr}^{-1}$ . The star formation

history of the satellites shows remarkable diversity: almost every galaxy is a special case (Grebel 1998; Mateo 1998). This diversity makes it very difficult to come up with a simple general model for formation of satellites in the Local Group. Because of the generally low star formation rates, it is not unexpected that the metallicities of the satellites are low: from  $\approx 10^{-2}$  for Draco and And III to  $\approx 10^{-1}$  for NGC 205 and Pegasus (Mateo 1998). There are indications that properties of the satellites correlate with their distance to the Milky Way (MW) or Andromeda, with dwarf spheroidals and dwarf ellipticals being closer to the central galaxy (Grebel 1997). Overall, about 40 satellites in the Local Group have been found.

Formation and evolution of galaxy satellites is still an open problem. According to the hierarchical scenario, small dark matter (DM) halos should on average collapse earlier than larger ones. To some degree, this is supported by observations of rotation curves of dark-matter dominated dwarfs and low-surface-brightness galaxies. The curves indicate that the smaller the maximum circular velocity, the higher the central density of these galaxies.

This is expected from the hierarchical models in which the smaller galaxies collapse earlier when the density of the Universe was higher (Kravtsov et al. 1998; Kormendy & Freeman 1998). Thus, it is likely that the satellites of the MW galaxy were formed before the main body of the MW was assembled. Some of the satellites may have survived the very process of the MW formation, whereas others may have been accreted by the MW or by the Local Group at later stages. Indeed this sequence forms the basis of the currently popular semi-analytical models of galaxy formation (e.g., Somerville & Primack 1998, and references therein).

There have been a number of efforts to use the Local Group as a cosmological probe. Peebles et al. (1989) modeled formation of the Local Group by gravitational accretion of matter onto two seed masses. Kroeker & Carlberg (1991) found pairs of “galaxies” in cosmological simulations and used them to estimate the accuracy of traditional mass estimates. Governato et al. (1997) studied the velocity field around Local Group candidates in different cosmological models and Blitz et al. (1998) simulated a group of galaxies and compared their results with the observations of the high-velocity clouds in the Local Group.

Nevertheless, despite significant effort, theoretical predictions of the abundance and properties of the satellites are far from being complete. One of the difficulties is the survival of satellites inside halos of large galaxies. This numerically challenging problem requires very high-resolution simulations in a cosmological context and has been addressed in different ways. In the classical approach (e.g., Lin & Lynden-Bell 1982; Kuhn 1993; Johnston et al. 1995), one assumes a realistic potential for the MW, a density profile for the satellites (usually an isothermal model with a central core), and numerically follows a satellite as it orbits around the host galaxy. This approach lends many valuable insights into the physical processes operating on the satellites and alleviates some of the numerical problems. It lacks, however, one important feature: connection with the cosmological background. The host galaxy is implicitly assumed to be stable over many billions of years which may not be realistic for a typical galaxy formed hierarchically. Moreover, the assumed isothermal density profile of the satellite is different from profiles of typical dark matter halos formed in hierarchical models (Navarro, Frenk & White 1997). Last but not least, the abundances of the satellites can only be predicted if the formation of the satellites and of the parent galaxy is modelled self-consistently. Thus, more realistic cosmological simulations are necessary.

Unfortunately, until recently numerical limitations prevented the usage of cosmological simulations to address satellite dynamics. Namely, dissipationless simulations seemed to indicate that DM halos do not survive once they fall into larger halos (e.g., White 1976; van Kampen 1995; Summers et al. 1995). It appears, however, that the premature destruction of the DM satellites inside the virial radius of larger halos was largely due to numerical effects (Moore, Katz, Lake 1996; Klypin et al. 1997 (KGKK)). Indeed, recent high-resolution simulations show that hundreds of galaxy-size DM halos do survive in clusters of

galaxies (KGKK; Ghigna et al. 1997; Colín et al. 1998). Encouraged by this success, we have undertaken a study of the survival of satellites in galaxy-size halos.

Dynamically, galactic halos are different from cluster-size halos (mass  $\gtrsim 10^{14}h^{-1} M_{\odot}$ ). Clusters of galaxies are relatively young systems in which most of the satellite halos have had time to make only a few orbits. Galaxies are on average significantly older, enabling at least some of their satellites to orbit for many dynamical times. This increases the likelihood of the satellite being destroyed either from numerical effects of the simulation or the real processes of dynamical friction and tidal stripping. The destruction of the satellites is, of course, counteracted by accretion of the new satellites in an ongoing process of galaxy formation. It is clear, therefore, that to predict the abundances and properties of galactic satellites, one needs to model self-consistently both the orbital dynamics of the satellites and the formation process of the parent halo in a cosmological setting. In this paper we present results from a study of galactic satellite abundances in high-resolution simulations of two popular variants of the Cold Dark Matter (CDM) models. As will be described below, the dissipationless simulations used in our study are large enough to encompass a cosmologically significant volume and, at the same time, have sufficient resolution to make the numerical effects negligible.

The paper is organized as follows. In §2 we present the data that we use to estimate the *observed* velocity function of satellites of our Galaxy and M31. Cosmological simulations are presented and discussed in §3. We compare the predicted and observed velocity functions in §4 to show that the models predict considerably more lower mass satellites than is actually observed in the Local Group. In §5 and 6 we discuss possible interpretation and implications of our results and summarize our conclusions.

## 2. SATELLITES IN THE LOCAL GROUP

There are about 40 known galaxies in the Local Group (Mateo 1998). Most of them are dwarf galaxies with absolute magnitudes of  $M_V \approx -10 - 15$ . While more and more galaxies are being discovered, most of the new galaxies are very small and faint making it seem unlikely that too many larger satellites have been missed. Therefore, we have decided to consider only relatively massive satellites with estimated rotational velocity or three-dimensional velocity dispersion of stars larger than 10 km/s. In order to simplify the situation even further, we estimate the number of satellites *per central galaxy*. There is a number of arguments why this is reasonable. First, it makes comparison with cosmological models much more straightforward. This is justified to some degree by the fact that the satellites in the Local Group cluster around either the MW or M31 and there are only a few very remote ones of unclear association with a central galaxy. We also believe that the estimate of the satellite abundance per galaxy is more accurate because it is relatively straightforward to find the volume of the sample, which would be more difficult if we were to deal with the Local Group as a whole<sup>1</sup>.

Using published results (Mateo 1998), we have compiled a list of satellites of the Milky Way and of the M31 with estimated circular velocities above the threshold of

<sup>1</sup>One of the problems would be choice of the outer boundary of the sample volume.

TABLE 1  
SATELLITES OF THE MW AND ANDROMEDA

$V_{\text{circ}}$ (km/s)	Milky Way 286/571kpc	Andromeda 286/571kpc	Average 286/571kpc	Comments
10	11 /13	13 /15	12/14	Sculptor Carina Sextans LeoII AndI-III,V,VI, CAS Pegasus
15	7 /9	7 /8	7/8.5	Phoenix Fornax LeoI UrsMin Draco Sagit Lgs3
20	2 /3	6 /7	4/5	IC1613
30	2 /3	6 /6	4/4.5	SMC NGC6822 IC10 NGC147 NGC185
50	1 /1	3 /3	2/2	LMC
70	0 /0	3 /3	1.5/1.5	M33 M32 NGC205

10 km/s. In our estimate of abundances, we have not attempted to decide whether a satellite is bound to its central galaxy or not. Satellites have been simply counted if they lie within a certain radius from the center of their parent galaxy. We have chosen two radii to make the counts. The counts of DM satellites were made for the same radii. The radii were chosen rather arbitrarily to be  $200h^{-1}$  kpc and  $400h^{-1}$  kpc. For a Hubble constant of  $h = 0.7$  ( $H_0 = 100h$  km/s/Mpc), which was assumed for our most realistic cosmological model and which is consistent with current observational results, the radii are 286 kpc and 571 kpc. The smaller radius is close to a typical virial radius of a Milky Way size halo in our simulations. The larger radius allows us to probe larger volumes (and, thus, gives better statistics) both in simulations and in observations. Unfortunately, observational data may become less complete for this radius.

Since we cannot estimate the luminosities of galaxies associated with DM satellites in dissipationless simulations, we have chosen circular velocity  $V_{\text{circ}}$  to characterize both the dark halos and the satellite galaxies. The circular velocity can be estimated for galaxies (with some uncertainties) and for the DM halos. For spiral and irregular galaxies we used the rotational velocity, which is usually measured from 21 cm HI observations. For ellipticals and dwarf spheroidals we used observed line-of-sight velocity dispersion of stars, which was multiplied by  $\sqrt{3}$  to give an estimate of  $V_{\text{circ}}$ . Using our numerical simulations we confirmed that this gives a reasonably accurate estimate of  $V_{\text{circ}}$  with an error less than  $\sim 10\% - 20\%$ . Table 1 lists the number of satellites with  $V_{\text{circ}}$  larger than a given value (first column) for the Milky Way galaxy (second column) and M31 (third column). The fourth column gives the average number of satellites and the fifth column lists names of the satellites in given velocity bin. Figures 4 and 5, discussed in detail below, present the cumulative circular velocity distribution of the observed satellites in MW and M31 within 286 kpc and 571 kpc radius from the central galaxies.

A few special cases should be mentioned. There are no measurements of velocity dispersion for AND I-III and the other two satellites of M31, AND V and VI, do not have measured magnitudes. Given that they all seem to have the properties of a dwarf spheroidal, we think it is reasonable to expect that they have  $V_{\text{circ}}$  in the range

10-20 km/s. Details of recent measurements of different properties of these satellites of the M31 can be found in Armandroff et al. (1998) and Grebel (1998). We also included CAS dSph (Grebel & Guhathakurta, 1998) in our list with  $V_{\text{circ}}$  in the range  $(10 - 20)$  km s $^{-1}$ . One satellite (AND II) can be formally included in both lists (MW and M31). It is 271 kpc from the M31, but being at the distance of 525 kpc from MW it should also be counted as the MW satellite. Since this is the only such case, we have decided to count it only once – as a satellite of M31.

### 3. COSMOLOGICAL MODELS AND SIMULATIONS

To estimate the satellite abundances expected in the hierarchical models, we have run simulations of two representative cosmologies. Parameters of the models and simulations are given in Table 2, where  $\Omega_0$  is the density parameter of the matter at  $z = 0$ ,  $\sigma_8$  is the rms of density fluctuations on  $8h^{-1}$ Mpc scale estimated by the linear theory at present time using the top-hat filter. Other parameters given in Table 2 specify the numerical simulations: mass of dark matter particle,  $m_{\text{particle}}$ , defines the mass resolution, number of time-steps at the lowest/highest levels of resolution, size of the simulation box, and the number of dark matter particles. Numbers on resolution refer to the size of the smallest resolution elements (cells) in the simulations.

The simulations have been performed using the Adaptive Refinement Tree (ART)  $N$ -body code (Kravtsov, Klypin & Khokhlov 1997). The ART code reaches high force resolution by refining the mesh in all high-density regions with an automated refinement algorithm. The  $\Lambda$ CDM simulation used here was used in Kravtsov et al. (1998) and we refer the reader to that paper for details and tests. Additional tests and comparisons with a more conventional AP $^3$ M code will be presented in Knebe et al. (1999). The CDM simulation differs from the  $\Lambda$ CDM simulations only in the cosmological parameters and size of the simulation box. Our intent was to use the much more realistic  $\Lambda$ CDM model for comparisons with observations, and to use the CDM model to test whether the predictions depend sensitively on cosmology and to somewhat broaden the dynamical range of the simulations. Jumping ahead, we note here that results of the CDM simulation are close to those of the  $\Lambda$ CDM simulation as far as the circular velocity function of satellites is concerned. This indicates

TABLE 2  
PARAMETERS OF SIMULATIONS

Model	$\Omega_0$	h	$\sigma_8$	$m_{\text{particle}}$ ( $h^{-1}M_\odot$ )	$N_{\text{steps}}$	Resolution ( $h^{-1}\text{pc}$ )	Box ( $h^{-1}\text{Mpc}$ )	$N_{\text{part}}$
SCDM	1.0	0.5	1.0	$2.05 \times 10^6$	650-40,000	150	2.5	$128^3$
$\Lambda$ CDM	0.3	0.7	1.0	$1.66 \times 10^7$	650-40,000	450	7.5	$128^3$

that we are dealing with general prediction of hierarchical scenarios, not particular details of the  $\Lambda$ CDM model. Nevertheless, we do expect that some details of statistics and dynamics of the satellites may depend on parameters of the cosmological models.

The size of the simulation box is defined by the requirement of high mass resolution and by the total number of particles used in our simulations. DM halos can be identified in simulations if they have more than  $\sim 20$  particles (KGKK). Small satellites of the MW and Andromeda have masses of  $\sim (1 - 5) \times 10^8 M_\odot$ . Thus, mass of a particle in the simulation should be quite small:  $\lesssim 10^7 M_\odot$ . Therefore, the number of particles in our simulations ( $128^3$ ) dictates the box size of only a few megaparsec across. This puts significant constraints on our results. The number of massive halos, for example, is quite small. In the CDM simulation we have only three halos with circular velocity larger than  $140 \text{ km s}^{-1}$ . The number of massive halos in the  $\Lambda$ CDM simulation is higher (eight).

The important issue for our study is the reliable identification of satellite halos. The problems associated with halo identification within high-density regions are discussed in KGKK. In this study we use a halo finding algorithm called Bound Density Maxima (BDM; see KGKK and Colín et al. 1998). The source code and description of the version of the BDM algorithm used here can be found in Klypin & Holtzman (1997). The main idea of the BDM algorithm is to find positions of local maxima in the density field smoothed at a certain scale and to apply physically motivated criteria to test whether the identified site corresponds to a gravitationally bound halo. The algorithm then computes various properties and profiles for each of the bound halos and constructs a uniform halo catalog ready to be used for analysis. In this study we will use the maximum circular velocity as the halo’s defining property. This allows us to avoid the problem of ambiguous mass assignment (see KGKK for discussion) and makes it easier to compare the results to observations.

The density maxima are identified using a top-hat filter with radius  $r_s$  (“search radius”). The search is performed starting from a large number of randomly placed positions (“seeds”) and proceeds by moving the center of mass within a sphere of radius  $r_s$  iteratively until convergence. In order to make sure that we use a sufficiently large number of seeds, we used the position of every tenth particle as a seed. Therefore, the number of seeds by far exceeds the number of expected halos. The search radius  $r_s$  also defines the minimum allowed distance between two halos. If the distance between centers of any of the two

halos is  $< 2r_s$ , only one halo (the more massive of the two) is left in the catalog. A typical value for the search radius is  $(5 - 10)h^{-1} \text{ kpc}$ . We set a lower limit for the number of particles inside the search radius  $N(< r_s)$ : halos with  $N(< r_s) < 6$  are not included in the catalog. We also exclude halos which have less than 20 bound particles and exclude halos with circular velocity less than  $10 \text{ km s}^{-1}$ . Some halos may have significant substructure in their cores due, for example, to an incomplete merger. Such cases appear in the catalogs as multiple (2-3) halos with very similar properties (mass, velocity, radius) at small separations. Our strategy is to count these as a single halo. Specific criteria used to identify such cases are: (1) distance between halo centers is  $\lesssim 30h^{-1} \text{ kpc}$ , (2) their relative velocity in units of the rms velocity of particles in the halos  $\Delta v/v$  is less than 0.15, and (3) the difference in mass is less than factor 1.5. If all the criteria are satisfied, only the most massive halo was kept in the catalog.

The box size of the simulations clearly puts limitations on sizes and masses of halos. In a few megaparsec box, one does not find large groups or filaments. The mean density in the simulation boxes, however, is equal to the mean density of the Universe, and thus we expect our simulations to be representative of the field population of galaxies (galaxies not in the vicinity of massive clusters and groups). The Local Group and field galaxies are therefore our main targets. Nevertheless, even in the small boxes used in this paper, the number of halos is very substantial. We find 1000 – 2000 halos of different masses and circular velocities in each simulation. This number is large enough for a reliable statistical analysis.

#### 4. SATELLITES: PREDICTIONS AND OBSERVATIONS

Figure 1 presents the velocity distribution function, defined as the number of halos in a given circular velocity interval per unit volume, in two  $\Lambda$ CDM simulations. The smaller-box simulation is the one that we use in our further analysis. To estimate whether the halo velocity function is affected by the small-box size, we compare the small-box result with results from the larger,  $60h^{-1} \text{ Mpc}$  box, simulation used in Colín et al. (1998). The latter followed the evolution of  $256^3$  particles and had a mass resolution of  $1.1 \times 10^9 h^{-1} M_\odot$ . In the small box, the total number of halos with  $V_{\text{circ}} > 10 \text{ km s}^{-1}$  and  $V_{\text{circ}} > 20 \text{ km s}^{-1}$  is 1716 (1066) for the lowest threshold of 20 bound particles. The numbers change slightly if a more stringent limit of 25 particles is assumed: 1556 (1052). In the overlapping range of circular velocities  $V_{\text{circ}} = (100 - 200) \text{ km s}^{-1}$  the velocity function of the small box agrees very well with that of the

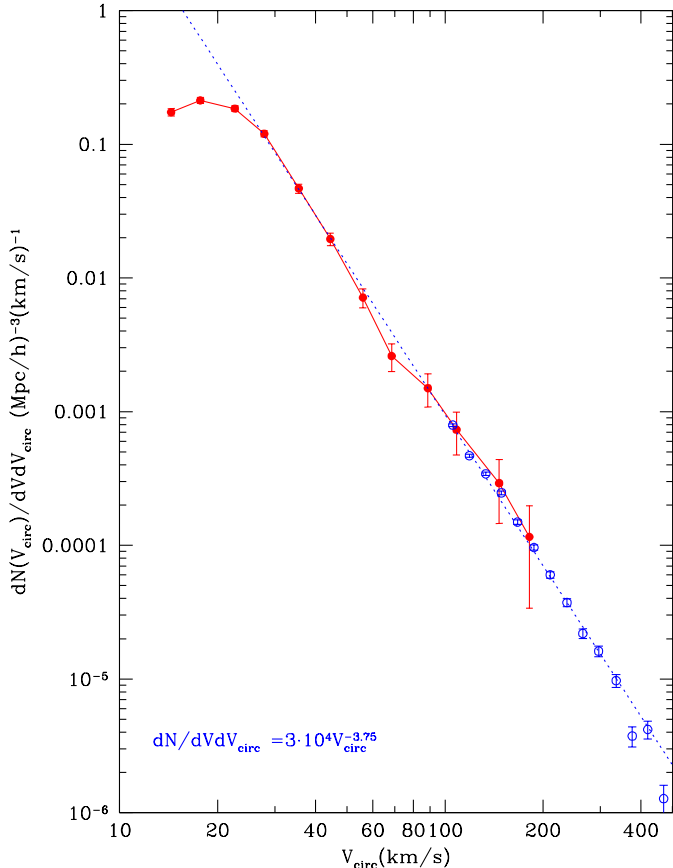


FIG. 1.— Differential circular velocity distribution function of dark matter halos in the  $\Lambda$ CDM model. The solid curve and the filled circles are results of the small-box (box-size of  $7.5h^{-1}\text{Mpc}$ ) simulation. Open circles show the corresponding velocity function in larger (box-size of  $60h^{-1}\text{Mpc}$ ) simulation. Error bars correspond to the Poisson noise. The dotted curve is the power-law with the slope of  $-3.75$  motivated by the Press-Schechter approximation (see §4 for details).

large box. This shows that the lack of long waves in the small-box simulation has not affected the number of halos with  $V_{\text{circ}} < 200 \text{ km s}^{-1}$ .

In the range  $V_{\text{circ}} \approx 20 - 400 \text{ km s}^{-1}$  the velocity function can be accurately approximated by a power law  $dN/dVdV_{\text{circ}} \approx 3 \times 10^4 V_{\text{circ}}^{-3.75} h^3 \text{Mpc}^{-3} / \text{km s}^{-1}$  motivated by the Press-Schechter (1974) approximation with assumptions of  $M \propto v^3$  and of the power-law power spectrum with a slope of  $n = -2.5$ . At higher circular velocities ( $V_{\text{circ}} > 300 \text{ km s}^{-1}$ ) the fit overpredicts the number of halos because the above fit neglects the exponential term in the Press-Schechter approximation. At small  $V_{\text{circ}} (< 20 \text{ km s}^{-1})$  the points deviate from the fit, which we attribute to the incompleteness of our halo catalog at these circular velocities due to the limited mass resolution. Indeed, comparison with the CDM simulation, which has higher mass resolution, shows that the number of halos increases by about a factor of three when the threshold for  $V_{\text{circ}}$  changes from  $20 \text{ km s}^{-1}$  to  $10 \text{ km s}^{-1}$ . We thus estimate the completeness limit of our simulations to be  $V_{\text{circ}} = 20 \text{ km s}^{-1}$  for the  $\Lambda$ CDM simulations and  $V_{\text{circ}} = 10 \text{ km s}^{-1}$  for the CDM run. Note that for the issue of satellite abundance discussed below, any incom-

pleteness of the catalogs at these velocities would increase the discrepancy between observations and models.

Figure 2 provides a visual example of a system of satellites around a group of two massive halos in the  $\Lambda$ CDM simulation. The massive halos have  $V_{\text{circ}} \approx 280 \text{ km s}^{-1}$  and  $\approx 205 \text{ km s}^{-1}$  and masses of  $1.7 \times 10^{12} h^{-1} M_{\odot}$  and  $7.9 \times 10^{11} h^{-1} M_{\odot}$  inside the central  $100h^{-1} \text{ kpc}$ . In Figure 3 the more massive halo is shown in more detail. To some extent the group looks similar to the Local Group though the distance between the halos is  $1.05h^{-1}\text{Mpc}$ , which is somewhat larger than the distance between the MW and M31. Yet, there is a significant difference from the Local Group in the number of satellites. In the simulation, there are 281 identified satellites with  $V_{\text{circ}} \gtrsim 10 \text{ km s}^{-1}$  within  $1.5 h^{-1}\text{Mpc}$  sphere shown in Figure 2. The Local Group contains only about 40 known satellites inside the same radius.

The number of expected satellites is therefore quite large. Note, however, that the total fraction of mass bound to the satellites is rather small:  $M_{\text{sat}} = 0.091 \times M_{\text{dm}}$ , where  $M_{\text{dm}} = 7.8 \times 10^{12} h^{-1} M_{\odot}$  is the total mass inside the sphere. Most of the mass is bound to the two massive halos. There is another pair of massive halos in the simulation, which has even more satellites (340), but the central halo in this case was much larger than M31. Its circular velocity was  $V_{\text{circ}} = 302 \text{ km s}^{-1}$ . We will discuss the correlation of the satellite abundances with the circular velocity of the host halo below (see Figs. 4 & 5). The fraction of mass in the satellites for this system was also small ( $\approx 0.055$ ).

Table 3 presents parameters of satellite systems in the  $\Lambda$ CDM simulation for all central halos with  $V_{\text{circ}} > 140 \text{ km s}^{-1}$ . The first and the second columns give the maximum circular velocity  $V_{\text{circ}}$  and the virial mass of the central halos. The number of satellites and the fraction of mass in the satellites are given in the third and fourth columns. All satellites within  $200$  ( $400$ )  $h^{-1} \text{ kpc}$  from the central halos, possessing more than 20 bound particles, and with  $V_{\text{circ}} > 10 \text{ km s}^{-1}$  were used. The last two columns give the three-dimensional rms velocity of the satellites and the average velocity of rotation of the satellite systems.

Figures 4 and 5 show different characteristics of the satellite systems in the Local Group (see §2), and in the  $\Lambda$ CDM and the CDM simulations. Top panels in the plots clearly indicate that the abundance and dynamics of the satellites depend on the circular velocity (and thus on mass) of the host halo. More massive halos host more satellites and the rms velocity of the satellites correlates with host's circular velocity, as can be expected. The number of satellites is approximately proportional to the cube of the circular velocity of the central galaxy (or halo):  $N_{\text{sat}} \propto V_{\text{circ}}^3$ . This means that the number of satellites is proportional to the galaxy mass  $N_{\text{sat}} \propto M$  because the halo mass is related to  $V_{\text{circ}}$  as  $M \propto V_{\text{circ}}^3$ . The number of the satellites almost doubles when the distance to the central halo increases by a factor of two. This is very different from the Local Group where the number of satellites increases only slightly with distance. Note that the fraction of mass in the satellites (see Table 3) does not correlate with the mass of the central object. The velocity dispersion decreases with distance, changing by 10% – 20% as

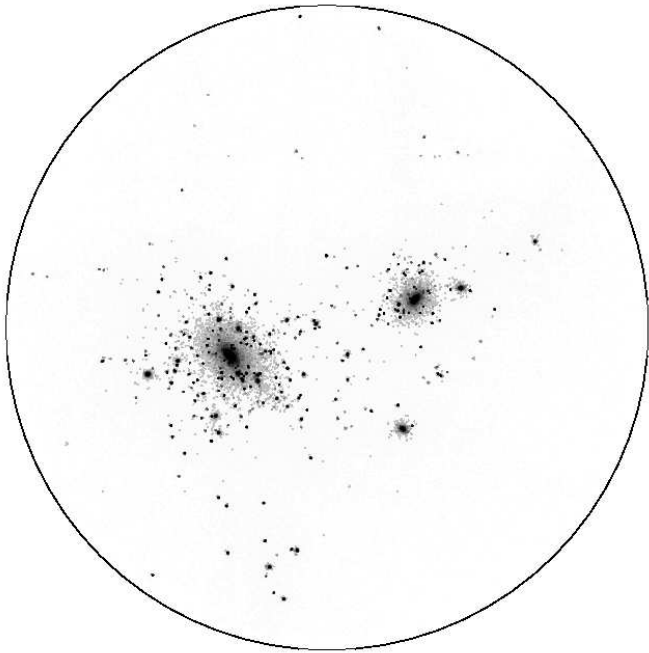


FIG. 2.— Distribution of dark matter particles inside a sphere of the radius of  $1.5h^{-1}\text{Mpc}$  (solid circle) for a small group of dark matter halos (similar in mass to the Local Group) in the  $\Lambda\text{CDM}$  simulation. The group consists of two massive halos with circular velocities of  $280\text{km s}^{-1}$  and  $205\text{km s}^{-1}$  (masses of  $1.7 \times 10^{12}h^{-1}M_{\odot}$  and  $7.9 \times 10^{11}h^{-1}M_{\odot}$  inside  $100h^{-1}$  kpc radius) and 281 halos with circular velocities  $> 10\text{ km s}^{-1}$  inside  $1.5h^{-1}\text{Mpc}$ . The distance between the halos is  $1.05h^{-1}\text{Mpc}$ . To enhance the contrast, we have color-coded DM particles on a grey scale according to their local density: intensity of each particle is scaled as the logarithm of the density, where the density was obtained using top-hat filter with  $2h^{-1}$  kpc radius.

the radius increases from  $200 h^{-1}$  kpc to  $400 h^{-1}$  kpc. We would like to emphasize that both the number of satellites and the velocity dispersion have large real fluctuations by a factor of two around their mean values.

The bottom panels in Figures 4 and 5 present the *cumulative* velocity distribution function (VDF) of satellites: the number of satellites per unit volume and per central object with internal circular velocity larger than a given value of  $V_{\text{circ}}$ . Note that the VDF is obtained as the unweighted average of the functions of individual halos in the interval  $V_{\text{circ}} \approx 150 - 300\text{ km s}^{-1}$ . This was done to improve the statistics. However, it is easy to check that the amplitude of the VDF corresponds to the satellite abundance around  $\approx 200\text{ km s}^{-1}$  halos. For instance, the average VDF shown in Figure 5 predicts  $\approx 50$  satellites within the radius of  $400h^{-1}$  kpc, while the upper panel of this figure shows that this is about what we observe for  $\approx 200\text{ km/s}$  hosts.

The right  $y$ -axis in the lower panels of Figures 4 and 5 shows the cumulative number of satellites in all host halos in the  $\Lambda\text{CDM}$  simulation. Error bars in the plots correspond to the Poisson noise. The dashed curve in Figure 5 shows VDF of all non-satellite halos (halos located *out-*

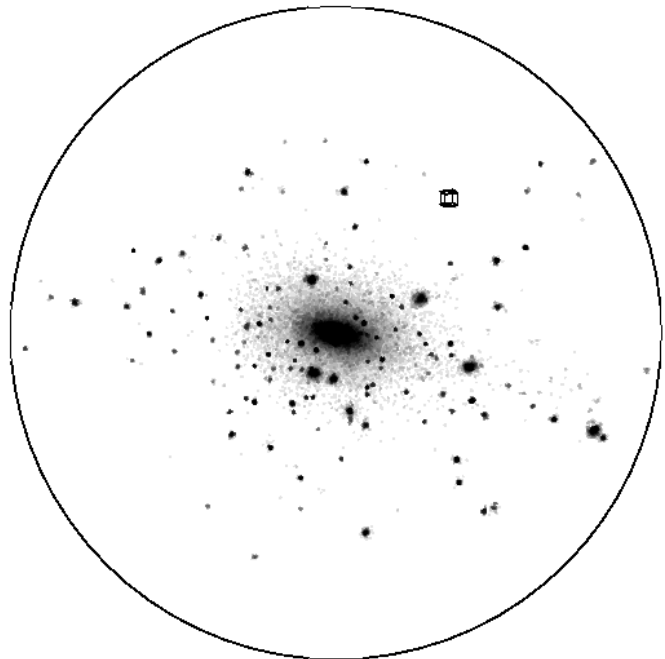


FIG. 3.— Distribution of dark matter particles inside a sphere of the radius of  $0.5h^{-1}\text{Mpc}$  (solid circle) centered on the more massive halo shown in Figure 2. The small box in the figure has size  $20h^{-1}$  kpc. The color-coding is similar to that in Figure 2 except that the local density was obtained using top-hat filter of  $3h^{-1}$  kpc radius.

*side*  $400 h^{-1}$  kpc spheres around the massive host halos). Comparison clearly indicates that the VDF of the satellite halos has the same shape as the VDF of the field halos with the only difference being the amplitude of the satellites' VDF. There are more satellites in the same volume close to large halos, but the fraction of large satellites is the same as in the field. We find the same result for spheres of  $200h^{-1}$  kpc radius.

The velocity distribution function can be roughly approximated by a simple power law. For satellites of the Local Group the fit at  $V_{\text{circ}} > 10\text{ km s}^{-1}$  gives

$$n(> V) = 300 \left( \frac{V}{10\text{ km s}^{-1}} \right)^{-1} (h^{-1}\text{Mpc})^{-3}, \quad (1)$$

and

$$n(> V) = 45 \left( \frac{V}{10\text{ km s}^{-1}} \right)^{-1} (h^{-1}\text{Mpc})^{-3}, \quad (2)$$

for  $R < 200 h^{-1}$  kpc and  $R < 400 h^{-1}$  kpc, respectively. For the  $\Lambda\text{CDM}$  simulation at  $V_{\text{circ}} > 20\text{ km s}^{-1}$  we obtain:

$$n(> V) = 5000 \left( \frac{V}{10\text{ km s}^{-1}} \right)^{-2.75} (h^{-1}\text{Mpc})^{-3}, \quad (3)$$

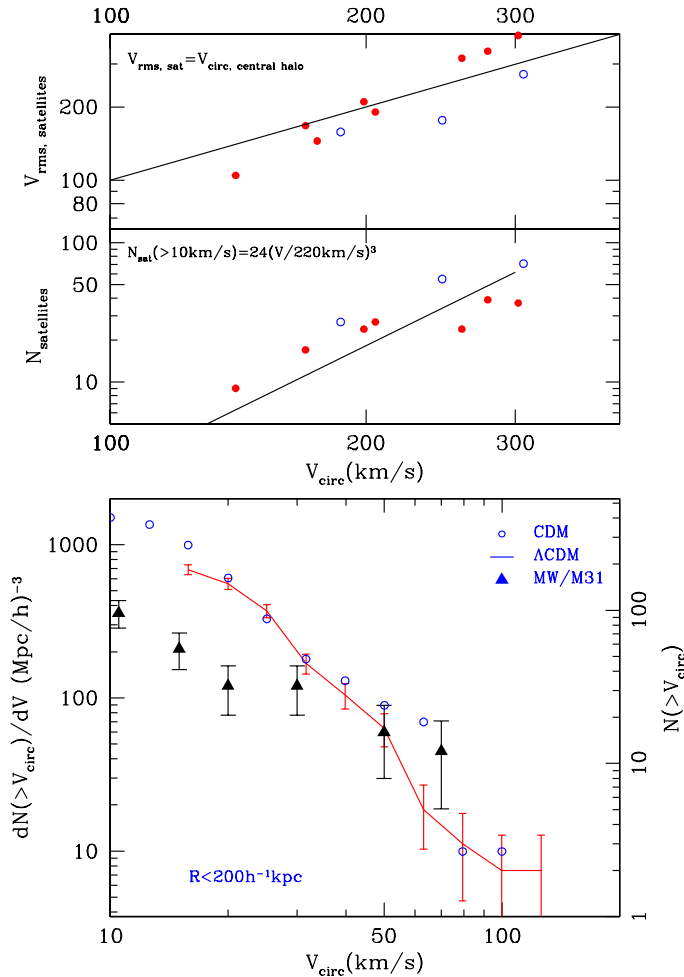


FIG. 4.— Properties of satellite systems within  $200 h^{-1}$  kpc from the host halo. *Top panel:* The three dimensional rms velocity dispersion of satellites versus maximum circular velocity of the central halo. *Solid* and *open* circles denote  $\Lambda$ CDM and CDM halos, respectively. The *solid line* is the line of equal satellite rms velocity dispersion and the circular velocity of the host halo. *Middle panel:* The number of satellites with circular velocity larger than  $10 \text{ km s}^{-1}$  versus circular velocity of the host halo. The *solid line* shows a rough approximation presented in the legend. *Bottom panel:* The cumulative circular velocity distribution (VDF) of satellites. *Solid triangles* show average VDF of Milky Way and Andromeda satellites. *Open circles* present results for the CDM simulation, while the *solid curve* represents the average VDF of satellites in the  $\Lambda$ CDM simulation for halos shown in the upper panels. To indicate the statistics, the scale on the right y-axis shows the total number of satellite halos in the  $\Lambda$ CDM simulation. Note that while the numbers of massive satellites ( $> 50 \text{ km s}^{-1}$ ) agrees reasonably well with observed number of satellites in the Local Group, models predict about five times more lower mass satellites with  $V_{\text{circ}} < 10 - 30 \text{ km s}^{-1}$ .

$$n(> V) = 1200 \left( \frac{V}{10 \text{ km s}^{-1}} \right)^{-2.75} (h^{-1} \text{Mpc})^{-3}, \quad (4)$$

again, for  $R < 200 h^{-1}$  kpc and  $R < 400 h^{-1}$  kpc, respectively. This approximation is formally valid for  $V_{\text{circ}} > 20 \text{ km s}^{-1}$ , but comparisons with the higher-resolution CDM simulations indicates that it likely extends to smaller

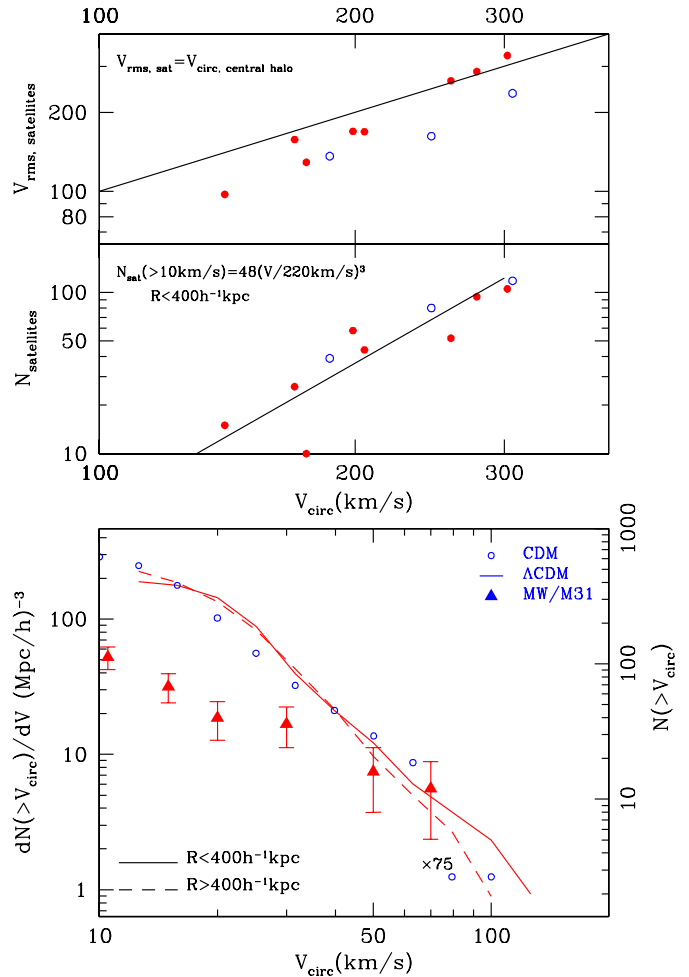


FIG. 5.— The same as in Figure 4, but for satellites within  $400 h^{-1}$  kpc from the center of a host halo. In the bottom panel we also show the cumulative velocity function for the field halos (halos outside of  $400 h^{-1}$  kpc spheres around seven massive halos), arbitrarily scaled up by a factor of 75. The difference at large circular velocities  $V_{\text{circ}} > 50 \text{ km s}^{-1}$  is not statistically significant. Comparison between these two curves indicates that the velocity functions of isolated and satellite halos are very similar. As for the satellites within central  $200 h^{-1}$  kpc (Figure 4), the number of satellites in the models and in the Local Group agree reasonably well for massive satellites with  $V_{\text{circ}} > 50 \text{ km s}^{-1}$ , but disagree by a factor of ten for low mass satellites with  $V_{\text{circ}} 10 - 30 \text{ km s}^{-1}$ .

velocities. The numbers of observed satellites and satellite halos cross at around  $V_{\text{circ}} = (50 - 60) \text{ km s}^{-1}$ . This means that while the abundance of massive satellites ( $V_{\text{circ}} > 50 \text{ km s}^{-1}$ ) reasonably agrees with what we find in the MW and Andromeda galaxies, the models predict an abundance of satellites with  $V_{\text{circ}} > 20 \text{ km s}^{-1}$  that is approximately five times higher than that observed in the

TABLE 3  
 SATELLITES IN  $\Lambda$ CDM MODEL INSIDE  $R = 200/400h^{-1}$  kpc FROM CENTRAL HALO

Halo $V_{\text{circ}}$ (km/s)	Halo Mass ( $h^{-1}M_{\odot}$ )	Number of satellites	Fraction of mass in satellites	$V_{\text{rms}}$ (km/s)	$V_{\text{rotation}}$ (km/s)
140.5	$2.93 \times 10^{11}$	9/15	0.053/0.112	99.4/94.4	28.6/15.0
278.2	$3.90 \times 10^{12}$	39/94	0.041/0.049	334.9/287.6	29.8/11.8
205.2	$1.22 \times 10^{12}$	27/44	0.025/0.051	191.7/168.0	20.0/11.3
175.2	$6.26 \times 10^{11}$	5/10	0.105/0.135	129.1/120.5	41.5/45.2
259.5	$2.74 \times 10^{12}$	24/52	0.017/0.029	305.0/257.3	97.1/16.8
302.3	$5.12 \times 10^{12}$	37/105	0.055/0.112	394.6/331.6	39.4/15.7
198.9	$1.33 \times 10^{12}$	24/58	0.048/0.049	206.1/169.3	17.7/12.1
169.8	$7.91 \times 10^{11}$	17/26	0.053/0.067	162.8/156.0	9.3/5.0

Local Group. The difference is even larger if we extrapolate our results to  $10 \text{ km s}^{-1}$ . In this case eq.(4) predicts that on average we should expect 170 halo satellites inside a  $200h^{-1}$  kpc sphere, which is 15 times more than the number of satellites of the Milky Way galaxy at that radius.

#### 5. WHERE ARE THE MISSING SATELLITES?

Although the discrepancy between observed and predicted satellite abundances appears to be dramatic, it is too early to conclude that it indicates a problem for hierarchical models. Several effects can explain the discrepancy and thus reconcile predictions and observations. In this section we briefly discuss two possible explanations: the identification of the missing DM satellites with High Velocity Clouds observed in the Local Group, and the existence of a large number of invisible satellites containing a very small amount of luminous matter either due to early feedback by supernovae or to heating of the gas by the intergalactic ionizing background.

##### 5.1. High Velocity Clouds?

As was recently discussed by Blitz et al. (1998), abundant High-Velocity Clouds (HVCs) observed in the Local Group may possibly be the observational counterparts of the low-mass DM halos unaccounted for by dwarf satellite galaxies. It is clear that not all HVCs can be related or associated with the DM satellites; there is a number of HVCs with a clear association with the Magellanic Stream and with the disk of our Galaxy (Wakker & van Woerden 1997; Wakker, van Woerden & Gibson 1999; and references therein). Nevertheless, there are many HVCs which may well be distant ( $> 100$  kpc; Wakker & van Woerden 1997; Blitz et al. 1998). According to Blitz et al., stability arguments suggest diameters and total masses of these HVCs of  $\sim 25$  kpc and  $3 \times 10^8 M_{\odot}$ , which is remarkably close to the masses of the overabundant DM satellites in our simulations.

The number of expected DM satellites is quite high. For the pair of DM halos presented in Figure 2, we have identified 281 DM satellites with circular velocities  $> 10$  km/s. Since the halo catalog is not complete at velocities  $\lesssim 20 \text{ km s}^{-1}$  (see §4), we expect that there should

be even more DM satellites at the limit  $V_{\text{circ}} = 10 \text{ km s}^{-1}$ . The correction is significant because about half of the identified halos have circular velocities below  $20 \text{ km s}^{-1}$ . Using eq.(3) we predict that the pair should host  $(280/2) \times 2^{2.75} = 940$  DM satellites with  $V_{\text{circ}} > 10 \text{ km s}^{-1}$  within  $1.5h^{-1}$  Mpc. A somewhat smaller number, 640 satellites, follows from eq.(4), if we double the number of satellites to take into account that we have two massive halos in the system.

The number of HVCs in the Local Group is known rather poorly. Wakker & van Woerden's (1991) all-sky survey, made with 1 degree resolution, lists approximately 500 HVCs not associated with the Magellanic Stream. About 300 HVCs have estimated linewidths (FWHM) of  $> 20 \text{ km s}^{-1}$  (see Fig.1 in Blitz et al.1998), the limit corresponding to 3D rms velocity dispersion of  $\sim 15 \text{ km s}^{-1}$ . Stark et al.(1992) found 1312 clouds in the northern hemisphere, but only 444 of them are resolved. The angular resolution of their survey was 2 degrees, but it had better velocity resolution than the Wakker & van Woerden compilation. Comparisons of low and high resolution observations indicates that the existing HVC samples are probably affected by selection effects (Wakker et al. 1999). The abundance of HVCs thus depends on one's interpretation of the data. If we take 1312 HVCs of Stark et al.(1992), double the number to account for missing HVCs in the southern hemisphere, we arrive at about 2500 HVCs in the Local Group. This is more than three times the number of expected DM satellites. This large number of HVCs also results in a substantial fraction of mass of the Local Group confined in HVCs. Assuming the average masses given by Blitz et al., this naive estimate gives the total mass in HVCs  $7.5 \times 10^{11} M_{\odot}$ . If we take mass of the Local Group to be  $\approx 3 \times 10^{12} h^{-1} M_{\odot}$  (Fich & Tremaine 1991), the fraction of mass in the HVCs is high: 0.2-0.25. This is substantially higher than the fraction of mass in DM satellites in our simulations ( $\approx 0.05$ ).

Nevertheless, there is another, more realistic in our opinion, way of interpreting the data. While it is true that Wakker & van Woerden (1991) may have missed many HVCs, it is likely that most of the missed clouds have small linear size. Thus, the mass should not be doubled when we make correction for missed HVCs. In this case 500 HVCs



(as in Wakker & van Woerden sample studied by Blitz et al.) with average dark matter mass of  $3 \times 10^8 h^{-1} M_\odot$  give in total  $1.5 \times 10^{11} h^{-1} M_\odot$  or 0.05 of the mass of the Local Group. This is consistent with the fraction of mass in DM satellites which we find in our numerical simulations. It should be kept in mind that the small HVCs may contribute very little to the total mass in the clouds.

As we have shown above, the number density of DM satellites is a very strong function of their velocity:  $dn(V)/dV \propto V^{-3.75}$ . If the cloud velocity function is as steep as that of the halos, this might explain why changes of parameters of different observational samples produce very large differences in the numbers of HVCs. The mass of a DM satellite is also a strong function of velocity:  $M \propto V^3$ . As the result, the total mass in satellites with velocity *less* than  $V$  is  $\propto V^{2.25}$ . The conclusion is that the mass is in the most massive and rare satellites. If the same is true for the HVCs, we should not double the mass when we find that a substantial number of small HVCs were missed in a catalog.

To summarize, it seems plausible that observational data on HVCs are compatible with a picture where every DM satellite either hosts a dwarf galaxy (a rare case at small  $V_{\text{circ}}$ ) or an HVC. This picture relies on the large distances to the HVCs and can be either confirmed or falsified by the upcoming observations (Wakker et al. 1999). Note, however, that at present the observed properties of HVCs (mainly the abundances, distances, and linewidths) are so uncertain that a more quantitative comparison is impossible.

### 5.2. Dark satellites?

There are at least two physical processes that have likely operated during the early stages of galaxy formation and could have resulted in the existence of a large number of dark (invisible) satellites. The first process is gas ejection by supernovae-driven winds (e.g., Dekel & Silk 1996; Yepes et al. 1997; Mac Low & Ferrara 1998). This process assumes at least one initial starformation episode, and thus should produce some luminous matter inside the host DM satellites. Indeed, this process may explain the observed properties of the dwarf spheroidal galaxies in the Local Group (e.g., Dekel & Silk 1996; Peterson & Caldwell 1993; Hirashita, Takeuchi & Tamura 1998). It is not clear whether this process can also produce numerous very low mass-to-light ratio systems missed in the current observational surveys. It is likely that some low-luminosity satellites have still been missed in observations, since several faint galaxies have been discovered in the Local Group just during the last few years (see §1). What seems unlikely, however, is that observations have missed so many. This may still be the case if missed satellites are very faint (almost invisible), but more theoretical work needs to be done to determine whether gas ejection can produce numerous very faint systems. The recent work by Hirashita et al. (1998) shows that this process may be capable of producing very high mass-to-light ratio ( $M/L$  up to  $\sim 1000$ ) systems of mass  $\lesssim 10^8 h^{-1} M_\odot$ .

Another possible mechanism is prevention of gas collapse into or photoevaporation of gas from low-mass systems due to the strong intergalactic ionizing background (e.g., Rees 1986; Efstathiou 1992; Thoul & Weinberg 1996; Quinn, Katz & Efstathiou 1996; Weinberg, Hernquist &

Katz 1997; Navarro & Steinmetz 1997; Barkana & Loeb 1999). Numerical simulations by Thoul & Weinberg (1996) and by Quinn et al. (1996) show that the ionizing background can inhibit gas collapse into halos with circular velocities  $\lesssim 30 \text{ km s}^{-1}$ . These results are in general agreement with more recent simulations by Weinberg et al. (1997) and Navarro & Steinmetz (1997).

As explained by Thoul & Weinberg, accretion of intergalactic gas heated by the ionizing background into dwarf  $\lesssim 30 \text{ km s}^{-1}$  systems is delayed or inhibited because the gas has to overcome pressure support and is, therefore, much slower to turn around and collapse. If the collapse may be delayed until relatively late epochs ( $z \lesssim 1$ ), many low-mass DM satellites may have been accreted by the Local Group without having a chance to accrete gas and form stars. This would clearly explain the discrepancy between the abundance of *dark matter* halos in our simulations and observed luminous satellites in the Local Group. More interestingly, a recent study by Barkana & Loeb (1999) shows that gas in small ( $V_{\text{circ}} \lesssim 20 \text{ km s}^{-1}$ ) halos would be photoevaporated during the reionization epoch even if the gas had a chance to collapse and virialize prior to that.

These results indicate that the ionizing background, of the amplitude suggested by the lack of the Gunn-Peterson effect in quasar spectra, can lead to the existence of numerous dark (invisible) clumps of dark matter orbiting around the Milky Way and other galaxies and thus warrants further study of the subject. It would be interesting to explore potential observational tests for the existence of dark satellites, given the abundances predicted in hierarchical models. One such feasible tests, examined recently by Widrow & Dubinski (1998), concerns the effects of DM satellites on microlensing statistics in the Milky Way halo.

## 6. CONCLUSIONS

We have presented a study of the abundance and circular velocity distribution of galactic dark matter satellites in hierarchical models of structure formation. Numerical simulations of the  $\Lambda$ CDM and CDM models predict that there should be a remarkably large number of dark matter satellites with circular velocities  $V_{\text{circ}} \approx 10 - 20 \text{ km s}^{-1}$  orbiting our galaxy – approximately a factor of five more than the number of satellites actually observed in the vicinity of the Milky Way or Andromeda (see §4). This discrepancy appears to be robust: effects (numerical or physical) would tend to produce more dark matter satellites, not less. For example, dissipation in the baryonic component can only make the halos more stable and increase their chance to survive.

Although the discrepancy between the observed and predicted satellite abundances appears to be dramatic, it is too early to conclude that it indicates a problem for hierarchical models. Several effects can explain the discrepancy and thus reconcile the predictions and observations. If we discard the possibility that  $\approx 80\%$  of the Local Group satellites have been missed in observations, we think that the discrepancy may be explained by (1) identification of the overabundant DM satellites with the High Velocity Clouds observed in the Local Group or by (2) physical processes such as supernovae-driven winds and gas heating by the ionizing background during the early stages of galaxy formation (see §5). Alternative (1) is attractive because the sizes, velocity dispersions, and abundance of the HVCs

appear to be consistent with the properties of the overabundant low-mass halos. These properties of the clouds are deduced under assumptions that they are located at large ( $\gtrsim 100$  kpc) distances which should be testable in the near future with new upcoming surveys of the HVCs. Alternative (2) means that the halos of galaxies in the Local Group (and other galaxies) may contain substantial substructure in the form of numerous invisible clumps of dark matter. This second possibility is interesting enough to merit further detailed study of the above effects on the

evolution of gas in low-mass dark matter halos.

We are grateful to Jon Holtzman and David Spergel for comments and discussions. This work was funded by the NSF grant AST-9319970, the NASA grant NAG-5-3842, and the NATO grant CRG 972148 to the NMSU. Our numerical simulations were done at the National Center for Supercomputing Applications (NCSA; Urbana-Champaign, Illinois).

## REFERENCES

- Armandroff, T.E., Davies, J.E., Jacoby, G.H. 1998, *AJ*, 116, 2287  
 Barkana, R., & Loeb, A. 1999, *ApJ*, submitted ([astro-ph/9901114](#))  
 Blitz, L., Spergel, D., Teuben, P., Hartmann, D., Burton, W.B., 1998, *ApJ*, submitted, [astro-ph/9803251](#)  
 Colin, P., Klypin, A.A., Kravtsov, A.V., Khokhlov, A.M. 1998, *ApJ*, submitted ([astro-ph/9809202](#))  
 Einasto, J., Lynden-Bell, D., 1982, *MNRAS*, 199, 67  
 Dekel, A., & Silk, J. 1986, *ApJ*, 303, 39  
 Efstathiou, G. 1992, *MNRAS*, 256, 43  
 Einasto, J., & Lynden-Bell, D. 1982, *MNRAS*, 199, 67  
 Fich, M., & Tremaine S. 1991, *ARA&A*, 29, 409  
 Ghigna, S., Moore, B., Governato, F., Lake, G., Quinn, T., Stadel, J. 1998, *MNRAS*, submitted ([astro-ph/9801192](#))  
 Governato, F., Moore, B., Cen, R., Stadel, J., Lake, G., Quinn, T., 1997, *New Astronomy*, 2, 91  
 Grebel, E.K. 1997, *Reviews of Mod. Astronomy*, 10, 29  
 Grebel, E.K. 1998, To appear in the proceedings of the XVIIIth Moriond conference on "Dwarf Galaxies and Cosmology", Les Arcs, March 1998, T. X. Thuan et al. (eds. ([astro-ph/9806191](#)))  
 Grebel, E.K., Guhathakurta, P. 1998, *ApJL*, 511, in press  
 Hirashita, H., Kamaya, H., & Takeuchi, T.T. 1998, *ApJ*, 504, L83  
 Irwin, M.J., Bunclark, P.S., Bridgeland, M.T., McMahon, R.G. 1990, *MNRAS*, 244, 16P  
 Johnston, K.V., Spergel, D., Hernquist, L., 1995, *ApJ*, 451, 598  
 Karachentseva, V.E., & Karachentsev, I.D. 1998, *A&AS*, 127, 409  
 Kauffmann, G., Nusser, A., & Steinmetz, M. 1997, *MNRAS*, 286, 795  
 Klypin, A.A., & Holtzman, J. 1997, preprint [astro-ph/9712217](#) (see also <http://astro.nmsu.edu/~aklypin/pmcode.html>)  
 Klypin, A.A., Gottlöber, S., Kravtsov, A.V., Khokhlov, A.M. 1998, *ApJ* accepted ([astro-ph/9708191](#)) (KGKK)  
 Knebe, A., Kravtsov, A.V., Gottlöber, S., Klypin, A.A. 1999, in preparation  
 Kormendy, J., & Freeman, K.C. 1998, *Bulletin AAS*, 193, 2105  
 Kravtsov, A.V., Klypin, A.A., Khokhlov, A.M. 1997, *ApJS*, 111, 73  
 Kravtsov, A.V., Klypin, A.A., Bullock, J.S., Primack, J.R. 1998, *ApJ*, 502, 48  
 Kroeker, T., & Carlberg, R., 1991, *ApJ*, 376, 1  
 Kuhn, J.R., 1993 *ApJ*, 409, L13  
 Lin, D.N.C., Lynden-Bell, D., 1982, *MNRAS*, 198, 707  
 Lynden-Bell, D., Cannon, R.D., Godwin, P.J. 1983, *MNRAS*, 204, 87  
 Mac Low, M.-M., & Ferrara, A. 1998, *ApJ*, submitted  
 Mateo, M.L. 1998, *ARA&A*, 36, 435  
 Moore, B., Katz, N., & Lake, G. 1996, *ApJ*, 457, 455  
 Navarro, J.F., Frenk, C., & White, S.D.M. 1997, *ApJ*, 490, 493 (NFW)  
 Navarro, J.F., & Steinmetz, M. 1997, *ApJ*, 478, 13  
 Peebles, P.J.E., Melott, A., Holmes, M., Jiang, L.R., 1989, *ApJ*, 345, 108  
 Peterson, R.C., & Caldwell, N. 1993, *AJ*, 105, 1411  
 Press, W.H., & Schechter, P. 1974, *ApJ*, 187, 425  
 Quinn, T., Katz, N., & Efstathiou, G. 1996, *MNRAS*, 278, P49  
 Rees, M.J. 1986, *MNRAS*, 218, 25  
 Somerville, R.S., & Primack, J.R. 1998, *MNRAS*, in press ([astro-ph/9802268](#))  
 Stark, A.A., Gammie, C.F., Wilson, R.W., Bally, J., Linke, R.A., Heiles, C., & Hurwitz, M. 1992, *ApJS*, 79, 77  
 Summers, F.J., Davis, M., & Evrard, A.E. 1995, *ApJ*, 454, 1  
 Thoul, A.A., & Weinberg, D.H. 1996, *ApJ*, 465, 608  
 van Kampen, E. 1995, *MNRAS*, 273, 295  
 Wakker, B.P., van Woerden, H. 1991, *A&A*, 250, 509  
 Wakker, B.P., van Woerden, H. 1997, *ARA&A*, 35, 217  
 Wakker, B.P., van Woerden, H., Gibson, B.K. 1999, to appear in *Stromlo Workshop on High Velocity Clouds*, B.K. Gibson and M.E. Putman (eds.), ([astro-ph/9901029](#))  
 Weinberg, D.H., Hernquist, L., Katz, N. 1997, *ApJ*, 477, 8  
 Whiting, A.B., Irwin, M.J., Hau, G.K.T. 1997, *AJ*, 114, 996  
 White, S.D.M. 1976, *MNRAS*, 177, 717  
 Weinberg, D., Hernquist, L., Katz, N., 1997, *ApJ*, 477, 8  
 Widrow, L.M., & Dubinski, J. 1998, *ApJ*, 504, 12  
 Yepes, G., Kates, R., Khokhlov, A., & Klypin, A. 1997, *MNRAS*, 284, 235  
 Zaritsky, D., Olszewski, E.W., Schommer, R.A., Peterson, R.C., Aaronson, M., 1989, *ApJ*, 345, 759  
 Zaritsky, D., White, S.D.M., 1994, *ApJ*, 435, 599  
 Zaritsky, D., Smith, R., Frenk, C., & White, S.D.M., 1997, *ApJ*, 478, 39